Zinc Oxide Nanowire Interphase for Enhanced Interfacial Strength in Lightweight Polymer Fiber Composites

Gregory J. Ehlert and Henry A. Sodano*

School of Mechanical, Aerospace, Chemical and Materials Engineering, Arizona State University, Tempe, Arizona 85287-6106

ABSTRACT A novel functionalization method for aramid fibers is developed to enhance the bonding of a ZnO nanowire interphase grown on the fiber surface for interfacial strength enhancement. The nanowire interphase functionally grades the typically discrete interface and reduces the stress concentration between the fiber and matrix. The functionalization process is developed to improve the bonding between the ZnO nanowires and the aramid fiber and is validated through Fourier transform IR and X-ray photoelectron spectroscopy studies. Mechanical testing shows significant improvement in the interfacial shear strength with no decrease in the base fiber strength. This is the only technique found in the literature for the growth of a nanowire interphase on polymer fibers for structural enhancement without degrading the in-plane properties of the bulk composite. Furthermore, it is firmly shown that the functionalization process is a necessary condition for enhanced interfacial strength, demonstrating that ZnO nanowires strongly interact with carboxylic acid functional groups.

KEYWORDS: ZnO nanowires • aramid • PPTA • functionalization • single-fiber fragmentation

INTRODUCTION

The future development of higher performance structures and systems depends heavily upon the employment of newer, lighter materials. Composite materials are an obvious choice because the constituents can be tailored to meet the structure's demands. In particular, a continuous fiber polymer matrix composite offers high strength to weight, high toughness to weight, and design flexibility to match the material with the structural demands. One fiber of commercial and academic interest is the aramid class of fibers (Kevlar and Twaron) because the highly crystalline structure offers one of the highest specific toughness ratios and the specific strength of common, commercially available fibers (1).

As our knowledge of composites has matured, the interface between the reinforcement and matrix has been a topic of great interest. The quality of the interface has been shown to be a crucial factor in many of the composite structure's bulk properties (2). Furthermore, a strong fiber and strong matrix may not necessarily result in a strong composite because the interface is equally important in determining the overall strength of the resulting material. As such, many prominent researchers have investigated methods for improving the interface of modern composite materials. Whiskerization (3−7), chemical treatment (8−21), and plasma treatment (22, 23) have all shown promising results for interface improvements; however, the fiber's mechanical properties are often significantly degraded, resulting in a composite with reduced in-plane properties.

Poly(*p*-phenyleneterephthalamide) (PPTA) or aramid fibers exhibit chemical resistance because of the high crystallinity of the fiber and the stability of the aromatic carbon atoms. While this property is advantageous in some instances, woven polymer matrix composites are often limited by a poor interface because the inert fiber will not react with the active groups of the polymer matrix. As such, many chemical treatments to change the surface groups of the aramid fiber have been attempted with limited success. Most of these chemical enhancements focused on the attachment of primary amine functional groups on the surface of the fiber because primary amines are one of the reactive constituents of thermoset epoxy polymer matrixes. Fibers have been functionalized by several processes including metalation−substitution, nitration−reduction, methylamine plasma functionalization, and ammonia plasma functionalization in the past with limited success. Several techniques have been employed to validate the surface chemistry such as X-ray photoelectron spectroscopy (XPS), IR studies, dye uptake methods, and elemental analysis.

Whiskerization or surface roughening has also been employed to enhance interfacial strength. Creating surface texture increases the surface area for van der Waals bonding and creates a strong mechanical interlock with the polymer matrix. Single-crystal silicon carbide or silicon nitride whiskers are grown on the surface of a fiber with great success in increasing the interfacial shear strength. Rabotonov et al. (3) noted that uniform spatial arrays of whiskers generated the highest improvements in interfacial strength. It was also

* E-mail: henry.sodano@asu.edu.
Received for review June 1, 2009 and accepted July 27, 2009
DOI: 10.1021/am900376t

noted, however, that the high temperatures and catalysts required for growth of the whiskers typically damaged the core fiber and reduced the in-plane strength of the composite. These investigations were performed on carbon fibers, which can withstand significantly higher temperatures than aramid or other polymer fibers. For this reason, no research on the whiskerization of polymer fibers occurs in the literature.

ZnO nanowire arrays have been frequently used for a wide range of applications ranging from power harvesting (24) to solar cells (25) to semiconductors (26). ZnO nanowire arrays have been employed for structural enhancement (7) by using the morphology of the nanowire array to interact with the matrix. In order for a nanowire interphase to enhance the interfacial interaction of a composite material, it must offer enhanced bonding with both the polymer matrix and the base fiber. The increased surface area and mechanical interlocking of the nanowire coating ensured and improved interaction with the polymer matrix while bonding with the base fiber. This reaction was hypothesized to be a result of the interaction of ZnO with functional oxide groups such as carboxylic acid. While the exact bonding has not been quantified, it is well-known that ZnO interacts strongly with carboxylic acid functional groups. The tetragonal bond angle of a free Zn^{2+} ion (109.5°) matches well with that of the sp_2-hybridized carbon atom (120°). Furthermore, in water the carboxylic acid group donates a proton to the solution and exhibits a negative charge, which coordinates with the Zn^{2+} ion through charge interaction. There have been several studies of how ZnO interacts with the carboxylic acid group; however, concise conclusions on the exact strength of such an interaction have yet to be determined (27).

A functionalization and ion-exchange technique is developed here that cleaves a portion of the polymer chains on the surface of the aramid fiber, resulting in a carboxylic acid group on the fiber. If the nanowire interphase is applied to the aramid fiber without a functionalization treatment, the interface between the nanowires and the fiber is weak and leads to reduced strength. The proposed technique will demonstrate the enhanced interaction of the ZnO coating with the functional groups and thus provide evidence of the dominant role of this interaction in nanowire interfaces. Additionally, the growth of secondary reinforcing materials on the surface of the polymer fibers has not been demonstrated in the literature because of the high-temperature (>600 °C) processing methods required in prior studies. The study will demonstrate a low-temperature method for the growth of a reinforcement on a polymer fiber and show the interphase results in improved interfacial strength, while preserving the tensile properties of the fiber. Furthermore, it will be shown that the functionalization process is a necessary condition for enhanced interfacial strength, demonstrating that ZnO nanowires strongly interact with carboxylic acid functional groups. To the best of our knowledge, the growth of a nano- or microstructured interface on a polymer reinforcing fiber has not been investigated in the literature nor has the use of a functionalization procedure to improve the bonding of the nanowires with the substrate, nor has the strong interaction between carboxylic acid and ZnO been quantitatively shown.

Fiber Functionalization and Nanowire Growth. Unidirectional aramid fibers were purchased from CST Sales (Tehachapi, CA). The aramid fibers were then washed in two successive chloroform baths followed by absolute ethanol to remove a manufacturer applied surface adhesive. The fibers were dried for 30 min under vacuum at 80 °C and then rinsed in acetone and ethanol to remove any further organic surface contaminants. Fibers were functionalized by soaking in a 10% aqueous NaOH solution that was cooled to 23 °C. Fibers were soaked for 20 min in an open beaker and then washed several times in large quantities of deionized water. Fibers were then dried for 60 min at 100 °C under a vacuum. An ion-exchange process was then performed on the functionalized fibers through an acid wash in a beaker of 33% HCl for 10 s and then rinsed several times in deionized water. The fibers were again dried at 100 °C for 60 min under a vacuum and mounted for XPS and FTIR analysis.

Seeds were synthesized by first creating a 0.02 M solution of NaOH in ethanol and a 0.0125 M solution of zinc acetate dihydrate in ethanol. Aliquots (80 mL) of the sodium hydroxide and zinc acetate solutions were then diluted with 200 and 640 mL of pure ethanol, respectively. The two solutions were heated to 55 °C separately, then mixed vigorously, and stirred continuously for 30 min. The seeds were then quenched in ice water to room temperature in order to slow the growth process. The cleaned, functionalized, dry fibers were dipped into the seeding solution, dried at room temperature, and then annealed at 150 °C to help adhere the seed layer for the ZnO nanowires. This was repeated two additional times, and then the fibers were placed into the ZnO growth solution. The growth solution is 0.025 M $Zn(NO_3)_2 \cdot 6H_2O$ and 0.025 M hexamethylenetetramine (Alfa Aesar, Ward Hill, MA) in deionized water at 90 °C. Fibers were placed in the preheated growth solution for 4 h in a temperature-controlled water bath and then gently washed several times in deionized water. Fibers were then dried at 100 °C under a vacuum and prepared for scanning electron microscopy (SEM) imaging.

A Bruker IFS 66 v5 vacuum spectrometer was used. Functionalized fibers were strung across a plate, and IR radiation was transmitted through a hole in the plate. The sample chamber was under a vacuum to reduce the effects of water and CO_2 on the data.

The XPS experiments were run at ultrahigh vacuum, $<10^{-8}$ Torr, with excitation from an Al Kα single anode source. The samples were mechanically mounted with a nonmagnetic mask, and charge compensation was performed with a 4 eV flood gun above the sample near the condenser lens. Machine control and data collection were performed with *Avantage* software, and data analysis, including peak decomposition, was performed in CASA XPS.

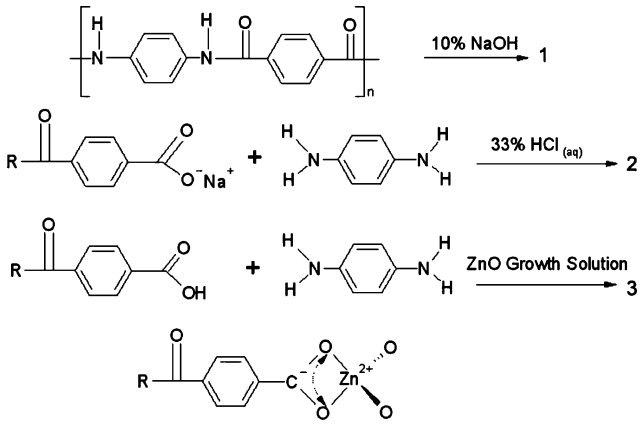

FIGURE 1. Functionalization reaction of aramid fibers through cleavage of the amide bond. First, the amide linkage is cleaved to create a carboxylate group and a primary amine group. The carboxylate group is then stripped of the Na^+ ion through an ion-exchange wash. Finally, the ZnO nanowire growth solution enables the carboxylic acid to act as an anchor site for a Zn^{2+} ion in the ZnO crystal.

Single-Fiber Characterization. Single fibers were separated and placed onto a paper template to create tabs. The fiber was attached to the tabs with epoxy and the gauge length between epoxy dots measured (~153 mm). An MTS Sintech 5G electromechanical tensile frame was used with a cross-head displacement rate of 1 mm/min. The load was measured with a 100 g load cell (Transducer Techniques, Temecula, CA) and displacement through the built-in cross-head position sensor.

Single-fiber segmentation testing was based upon the detailed work of Feih et al. (34) Single aramid fibers were placed in a silicone rubber mold (3120 RTV; Dow Corning, Midland, MI) and pretensioned to 15 g. The molds were then filled with a 100:16.9 mixture of Epon 862/Epikure 9553 (Hexion, Houston, TX) and gelled for 1 h. The molds were heated in an oven to 100 °C for 1 h, followed by 1 h at 160 °C. Samples were polished and then observed during the tensile straining in a microscope with transmitted polarized light. Samples were strained and then scanned for cracks until the number of cracks in the length of the fiber was saturated.

RESULTS AND DISCUSSION

During our development of the ZnO nanowire interface for polymer fiber composites, it was found that the adhesion between the inorganic nanowires and the organic aramid fiber was very weak. Through a competitive growth process, the ZnO nanowires grow with vertical alignment, which results in the formation of a thin film of ZnO between the nanowires and the polymer fiber. Under poor adhesion, this morphology results in the nanowires falling off in sheets. To alleviate this issue, a fiber functionalization procedure was employed to enhance the interaction of the ZnO nanowires with the highly crystalline aramid fiber. The functionalization procedure first splits the amide linkage of the aramid backbone chain to create a carboxylate group and a primary amine (9, 12), as shown in Figure 1. Following cleavage of the amide linkage, sodium ions are left on the carboxylate

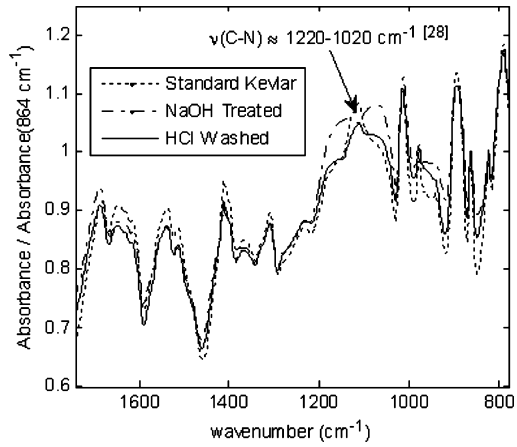

FIGURE 2. Reduced absorbance of C−N stretching due to cleavage of the amide linkage during functionalization.

functional groups. This reaction has been validated through the use of diffuse-reflectance IR spectroscopy (9, 28, 29) and results in only a fraction of the surface chains being broken, as will be shown in our XPS data. To use the carboxylic acid functional group to create a chemical bond between the ZnO nanowires and the polymer fiber,the sodium ions were removed through an ion-exchange wash developed for this application and shown in the later half of the functionalization procedure. Additionally, excess metal ions were found to contaminate the growth solution, making their removal necessary. This ion-exchange wash uses a high concentration of hydrogen ions in the HCl to force the sodium ions into solution, leaving carboxylic acid groups in its place, as shown from steps 2 to 3 in Figure 1. Once the fibers are then placed into the aqueous nanowire growth solution, the carboxylic acid group donates a proton to the solution and exhibits a negative charge, which coordinates with the Zn^{2+} ion. The chemisorption of ZnO with the carboxylic acid group has been demonstrated through spectroscopic studies of the adsorption of formic acid onto ZnO. This functionalization procedure will be shown to significantly enhance the growth of the ZnO nanowires on the surface of the highly crystalline aramid fiber.

Transmitted IR studies were performed to validate the chemical-bonding structure of the fibers. The characteristic absorbances were collected in the IR range from 4000 to 400 cm^{-1} and will be sensitive to organic carbon bonds (30). In order to account for slight sample-to-sample variations in the signal intensity, absorbance spectra were normalized by an absorbance at 864 cm^{-1}, consistent with the literature (9). It is observed in Figure 2 that the peak corresponding to C−N absorption (30), ~1110 cm^{-1}, was reduced in relative intensity following the sodium hydroxide treatment. Sodium hydroxide is a well-known catalyst for hydrolysis of the amide bond, and the reaction conditions are not suitable for an aromatic substitution reaction (31). As such, the reduced absorption is attributed to the reaction and creation of surface functional groups. Because the reaction conditions are quite mild for only a brief time, the reaction is presumed to occur mainly on the surface and not to progress to completion. Because FTIR is a transmission technique,

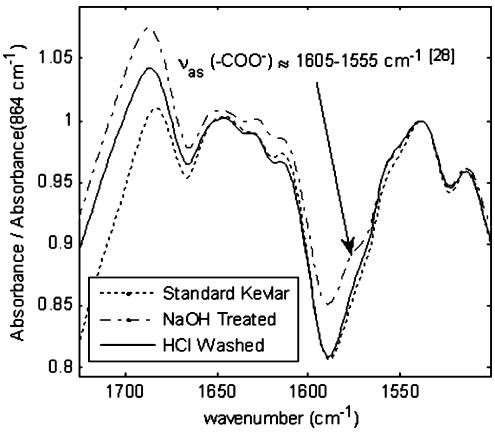

FIGURE 3. Absorbance of a carboxylate salt group on functionalized aramid fibers. The indicated shoulder corresponds to antisymmetric stretching of the $-COO^-$ bond.

signals are averaged over the entire volume of the sample, and thus only the small portion of polymer chains on the fiber surface that are broken result in a relatively weak modification of the IR, as can be seen in Figure 2. However, variation in the IR signal measured was found to be repeatable.

After the initial hydrolysis of the peptide bond, a carboxylate salt remained instead of the desired carboxylic acid group. It was observed that carboxylate groups did not encourage or even permit the attachment of ZnO nanowire arrays. This was attributed to the presence of the Na^+ ion at the bonding site of the carboxylic acid group or the contamination of the growth solution by Na^+ ions. The ion-exchange wash was developed to remove the Na^+ ions without catalyzing the condensation reaction, which might reverse the functionalization. A strong acid is chosen in order to increase the concentration of free protons to replace the missing Na^+ ions. Because acids also catalyze the hydrolysis of peptide bonds, reversal of the functionalization is not expected to occur. A 33% HCl solution ion-exchange wash is shown to remove the carboxylate salt absorbance (28) created during functionalization. Figure 3 shows an increase of the carboxylate absorbance after functionalization followed by a return to as-received levels after the acid wash, validating that the acid wash is effective in removing Na^+ contamination.

XPS provides analysis of the surface functional groups by analyzing the bonding states of the atoms present on the surface of the sample. The broad spectral analysis of the fibers will indicate the surface composition of the fibers. Aramid fibers, as received, have three bonding states of carbon, one bonding state of nitrogen, and one bonding state of oxygen. The chemical functionalization treatment should create one new state of each carbon, oxygen, and nitrogen; thus, four carbon, two oxygen, and two nitrogen peaks are fit to each high-resolution scan of each element. In order to validate the chemical treatment and surface functionality, the hypothesized C 1s peaks must be listed and compared to collected spectra. It is expected that carbon, oxygen, and nitrogen will all be present and most other elements will not be present, specifically, sodium, which

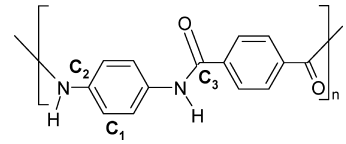

FIGURE 4. Carbon states in aramid fibers, as received.

should be removed by the ion-exchange wash. The aromatic carbon state, C1, theoretically appears 10 times per monomer in Figure 4, which should yield an area fraction of $^{10}/_{14}$ or 71.4%. C2 occurs two times per monomer and should show $^{2}/_{14}$ or 14.3%; C3 should also appear one-fifth as often as C1, occurring twice. Furthermore, the creation of a new bonding state corresponding to a carboxylic acid could occur as many as two times per monomer unit for full progression of the reaction. Because the carboxylic acid groups are all from hydrolyzed amide links, the concentrations of the carboxylic acid groups and the amide links (two carbons per monomer) should sum to the concentrations of the aromatic substituted carbons (two carbons per monomer), which are not expected to be affected by the functionalization procedure.

One particularly important aspect of performing an XPS study on insulating polymeric samples is the accumulation of surface charge. Because the sample accepts an X-ray (zero charge) and emits an electron (1− charge), the sample will accumulate a positive charge. This charge will help to restrain the electron, and electrons of a higher energy will be emitted and detected. The peaks of the sample collected will be shifted, sometimes by a few electronvolts or by as many as 50−100 eV in extreme cases. Techniques have been developed to compensate for this such as the use of conductive masks or low-energy electron flood guns (32). The first technique employed on this sample was to place a mask consisting of a metallic sheet with a small hole in it over the fibers to maximize contact with the ground path. Second, we employed an electron flood gun, a low-energy (4 eV) electron emitter that drops electrons on the surface from above the collection lenses to compensate for the charge. The spectra were also minimally corrected based on the well-established value for the binding energy (32) of an aromatic carbon; specifically, the largest peak center was shifted to 284.7 eV. The peaks were then analyzed for spread (full width at half-maximum) and center location.

The collected spectra of intensities at various binding energies are decomposed into a sum of Gaussian−Lorentzian distributions centered at various locations. A Shirley background was subtracted, and the peaks decomposed, as shown in Figure 5. Peak labels were introduced to show the chemical bonding state associated with the particular carbon. Four individual peaks best matched the collected data in the carbon region on the functionalized fiber, which is also consistent with the theorized number. The peak locations align fairly well with values presented by Beamson and Briggs (32) in their analysis of the bonding states of various polymers. The broad elemental composition scan indicated that the fiber had only carbon, oxygen, and nitrogen present, which was consistent with the theorized hydrolysis reaction and ion-exchange wash.

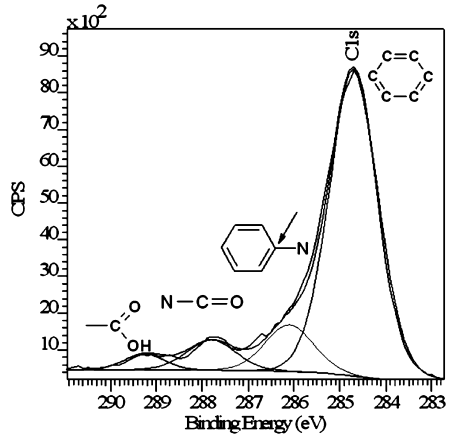

FIGURE 5. Decomposed bonding states of the C 1s energy region with labeled chemical structures, showing the presence of functional groups on the aramid fiber surface. Table 1 shows the relative fraction of each state.

Table 1. Theoretical and Experimental Bonding State Peak Locations and Concentrations Showing Excellent Agreement between Peak Locations and Published Values[a]

Chemical Structure	Peak Location (eV)	Peak Fit (eV)	Error (eV)	Theor. State Conc.	Meas. State Conc.
—C(=O)—OH	289.18 289.33	289.25	0.07 -0.08	0.0%	3.24%
N—C=O	287.97 288.59	287.8	-0.17 -0.79	14.3%	7.61%
	284.7	284.7	0	71.4%	77.5%
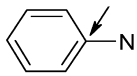	285.94	286.1	0.16	14.3%	11.7%

[a] The stated concentrations of the carboxylic acid and the amide bond sum to the concentration of aromatic substituted carbons, which is consistent with the proposed reaction.

As can be seen in Table 1, the peak fit locations align remarkably well. The largest peak, aromatic carbon, was aligned to match the literature value (32) and compensate for the charging, thus showing no error. The charging difference is expected to be nominally the same on all electrons, and so all peaks are shifted by the same amount. In order to validate the reaction and ensure that the carboxylic acid groups are not from contamination, the state concentrations must be compared. It is theorized in Figure 1 that the functionalization reaction splits the amide linkage while preserving the aromatic amine group. The concentration of aromatic amines is expected to remain constant, and the sum of the carboxylic acid groups and amide linkages should remain equal to that of the aromatic amine concentration. While a higher concentration of aromatic carbons is observed, the sum of the carboxylic acid groups and amide linkages (10.9%) is very close to that of the aromatic amine (11.7%). Furthermore, the general concentrations are approximately correct, which further validates the conclusions of the functionalization. Table 1 shows that amide linkages are still present, showing that only a limited fraction of the surface polymer chains are broken and the mechanical properties are not expected to be degraded.

The ZnO nanowire arrays on aramid fibers can be seen in Figure 6A. The nanowires are relatively uniform in length and diameter and grow from the thin film seed layer, as shown in Figure 6A, inset. A typical nanowire is about 100 nm in diameter and 3.5 μm in length. The growth process often precipitates large crystalline prisms on the fibers or fabrics; however, the prisms are very large and are not bonded strongly to the fibers. The gentle washing procedure attempts to remove most of the crystals, but some still remain, which can be seen in the SEM micrograph in Figure 6A. The as-received fibers exhibit large adhesive failure of the nanowire arrays in Figure 6B, which is due to the lack of proper functional groups for ZnO to bond to. The inert chemical behavior of aramid fibers was observed to be detrimental; however, this was overcome with the functionalization procedure, as Figure 6A indicates. Figure 6C shows the wurtzite structure of the ZnO nanowires, with well-aligned peaks to the standard in the literature (33).

The ZnO nanowires interphase is designed to significantly improve the interfacial strength in aramid fibers; however,

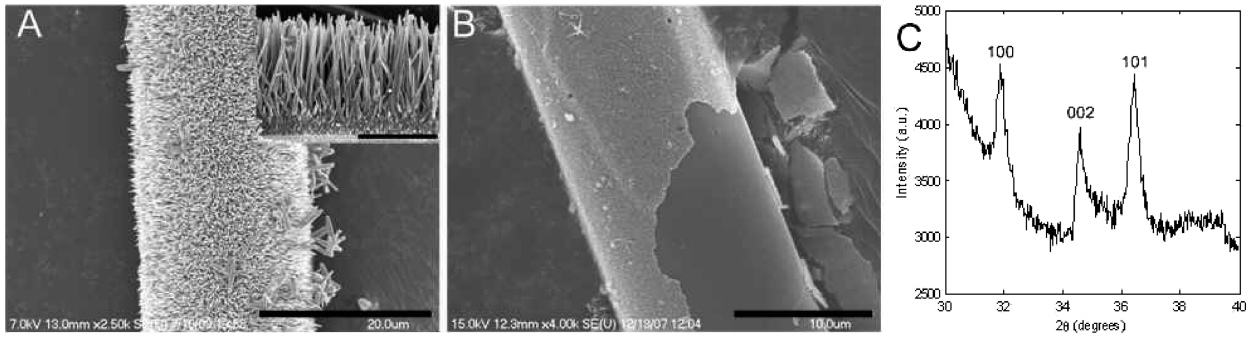

FIGURE 6. (A) SEM micrograph of aligned ZnO nanowire arrays grown on carboxylic acid functionalized aramid fibers (scale bar 20 μm). The upper inset shows a cross section of ZnO nanowires grown from the randomly oriented seed layer and aligned by competitive growth (scale bar 3 μm). The nanowires are rather uniform in diameter, ~100 nm, and length, ~3.5 μm. (B) SEM micrograph of ZnO nanowires falling off of an as-received aramid fiber. The inert surface prevents adhesion of the nanowires to the fiber and indicates the need for a functionalization procedure (scale bar 10 μm). (C) X-ray diffraction pattern of ZnO nanowires grown on aramid fibers showing the standard wurtzite crystal structure (*33*).

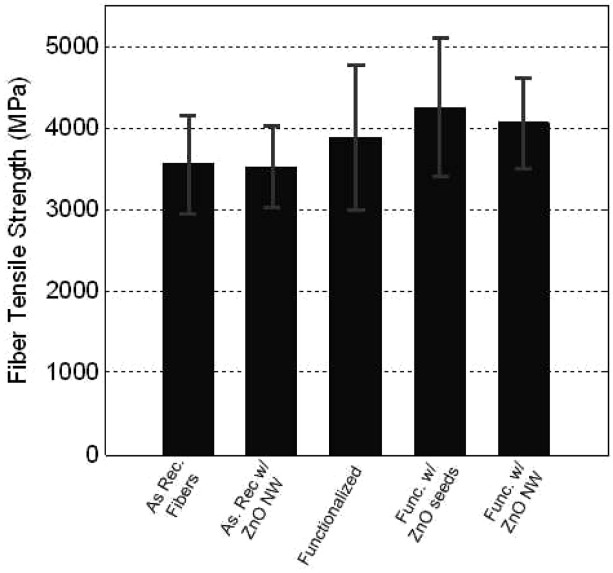

FIGURE 7. Tensile strength of modified aramid fibers showing no degradation in the fiber tensile strength. The fibers tested were as-received, as-received with ZnO nanowires, functionalized fibers, functionalized with ZnO seeds, and functionalized with ZnO nanowires.

to be effective, it must also preserve the fiber properties so that the composite's in-plane properties are maintained. In order to demonstrate this, single-fiber tensile testing has been performed to characterize the in-plane strength, which is dominated by the fiber's axial properties. The results of the single-fiber tensile strength are shown in Figure 7. It can be seen in this figure that the strength of the fiber is not negatively influenced by either the functionalization or nanowire growth processes. This result is a major advantage of this work because past efforts for chemical modification of the fiber surface to achieve increased adhesion with the matrix have all seen improved interfacial properties at the cost of the fiber strength. No other current whiskerization technique is compatible with polymer fibers because of the high-temperature processing required. Because our growth process is performed at 90 °C, which is well below the temperature at which aramid fiber degrades at, nanowire growth does not affect the fiber integrity. It should be noted that the strength of the fiber slightly increases following functionalization, which is attributed to removal of the weak outer layer of the fiber during functionalization. This result demonstrates that neither the functionalization nor growth processes will negatively impact the in-plane properties of the composite.

Following the evaluation of the fiber properties, the interfacial properties of the fiber after surface treatment can be evaluated through single-fiber fragmentation, which is widely used for interfacial strength assessment (34). The single-fiber fragmentation test measures the saturated critical length of fibers embedded in a large polymer matrix. For a given gauge section, the average critical length is inversely proportional to the number of cracks observed and the average critical length is inversely proportional to the interfacial strength; thus, the number of cracks is proportional to the interfacial strength. The tensile testing system for single-fiber fragmentation testing was designed such that it allows the stress and strain on the specimen to be applied and monitored through an optical microscope under polarized light. The samples were placed in a screw-driven microtensile test stage shown in Figure 8a. Using this system, the number of fragments was measured under increasing strain such that the saturation point could be identified. Figure 8b shows an optical micrograph of the fractured fiber. The number of fragments was then used to determine the critical length and interfacial strength of the composite (34). Segmentation tests were performed on bare and functionalized aramid fibers as well as bare and functionalized fibers with ZnO nanowires grown on the surface. The interfacial shear strength for each of the four cases studied is plotted in Figure 8a. The interfacial shear strength values observed of bare, as-received, fibers are comparable to those presented in single-fiber fragmentation testing in the literature (13). The interfacial strength of the functionalized fiber with ZnO nanowires is observed to increase 51% over that of the as-received fibers. It is expected that carboxylic acid groups will not interact with the epoxide or amine groups of the bisphenol F epoxy resins used here, and

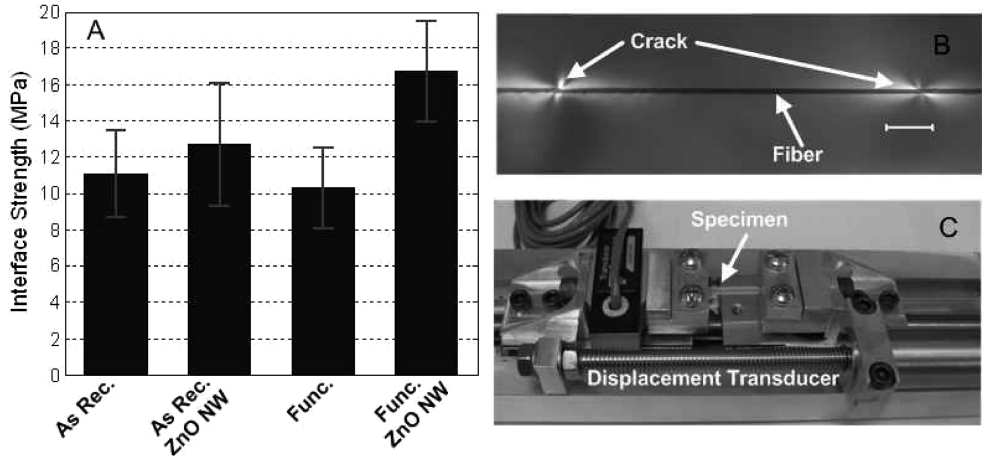

FIGURE 8. Single-fiber segmentation results (A) showing a 51% improvement in the single-fiber interfacial strength. The four fibers tested were as-received, as-received with ZnO nanowires, functionalized, and functionalized with ZnO nanowires. (B) Micrograph of the typical fiber cracks as observed in situ during the test (scale bar 100 μm). (C) Microtensile frame used in the testing with a specimen in jaws.

thus the functionalization procedure does not increase the interfacial strength over that of the bare fibers. The single-fiber fragmentation data also show that, without functionalization, the nanowires only lead to a marginal interfacial strength increase. This demonstrates that the addition of carboxylic acid functional groups on the fiber surface is critical for the strong adhesion of the ZnO nanowires on the surface of the fiber. The growth of a ZnO nanowire interphase creates two interfaces, one between the aramid and ZnO and one between ZnO and the epoxy. The increased interfacial strength indicates that both interfaces are stronger than the aramid−epoxy adhesion. The demonstration that ZnO strongly bonds with carboxylic acid is new to the literature and could be used to increase the strength of other interfaces between organic and inorganic materials.

CONCLUSIONS

A novel ZnO nanowire interfacial treatment has been developed for aramid fiber reinforced composites. The ZnO nanowire interphase leads to a significantly increased surface area for bonding as well as mechanical interlocking with the polymer matrix to enhance load transfer. However, it was found that the ZnO nanowires grown on an aramid fiber had poor adhesion to the fiber, which resulted in no interfacial strength increase. The application of an interphase creates two interfaces, both of which must be stronger than the original to achieve increased strength. To address the weak adhesion between the fiber and nanowires, a functionalization and ion-exchange procedure was developed to produce carboxylic acid groups on the surface fiber. It was quantitatively demonstrated that the addition of carboxylic acid functional groups on the fiber surface is critical for the strong adhesion of the ZnO nanowires; following functionalization, the ZnO nanowires led to a 51% increase in the interfacial strength. It was also demonstrated that the low temperatures required for growth of the ZnO nanowires did not degrade the fiber strength as prior interfacial enhancement methodologies have. No whiskerization techniques compatible with polymer fibers were found in the literature, which indicates that this novel procedure could lead to numerous advances in smart and nanostructured interfaces. Furthermore, the piezoelectric and semiconductive properties of ZnO could lead to multifunctional composites with embedded sensing, actuation, or power harvesting properties.

Acknowledgment. The authors gratefully acknowledge Dr. R. Brett Williams for help with the mechanical testing, Dr. Dong-Kyun Seo for assistance with functionalization, Ken Mossman for assistance with FTIR, and Tim Karcher for assistance with XPS. We also acknowledge the LeRoy Eyring Center for Solid State Science and NASA Jet Propulsion Laboratory (Award 1340346).

REFERENCES AND NOTES

(1) Daniel, I.; Ishai, O. *Engineering Mechanics of Composite Materials*, 2nd ed.; Oxford University Press: New York, 2006.
(2) Hyer, M.; White, S. *Stress Analysis of Fiber-reinforced Composite Materials*, 1st ed.; McGraw-Hill: New York, 1997.
(3) Rabotnov, J.; Perov, B.; Lutsan, V.; Ssorina, T.; Stepanitsov, E. *Carbon Fibers—Their Place in Modern Technology*; The Plastics Institute: London, 1974; p 65.
(4) Kowbel, W.; Bruce, C.; Withers, J.; Ransone, P. *Composites, Part A* **1997**, *28A*, 993–1000.
(5) Thostenson, R.; Li, E.; Wang, W.; Ren, Z.; Chou, T. *J. Appl. Phys.* **2002**, *91*, 6034–6037.
(6) Bekyarova, E.; Thostenson, E.; Yu, A.; Kim, H.; Gao, J.; Tang, J.; Hahn, T.; Chou, T.; Itkis, M.; Haddon, R. *Langmuir* **2007**, *23*, 3970–3974.
(7) Lin, Y.; Ehlert, G.; Sodano, H. *Adv. Funct. Mater.* **2009**, in press.
(8) Gardner, S.; Singamsetty, C.; Wu, Z.; Pittman, C. *Interface Anal.* **1996**, *24*, 311–320.
(9) Chatzi, E.; Tidrick, S.; Koenig, J. *J. Polym. Sci., Part B: Polym. Phys.* **1988**, *26*, 1585–1593.
(10) Park, S.; Seo, M.; Ma, T.; Lee, D. *J. Colloid Interface Sci.* **2002**, *252*, 249–255.
(11) Clark, D.; Feast, W. *Polymer Surfaces*; John Wiley & Sons: New York, 1978; pp 309−351.
(12) Keller, T.; Hoffman, A.; Ratner B.; McElroy, B. In *Physiochemical Aspects of Polymer Surfaces*; Mittal, K., Ed.; Plenum University Press: New York, 1981; Vol. 2, pp 861−879.
(13) Kalantar, J.; Drzal, L. *J. Mater. Sci.* **1990**, *25*, 4186–4202.
(14) Penn, L.; Wang, H. *Polym. Adv. Technol.* **1994**, *5*, 809–817.
(15) Lin, J.-S. *Eur. Polym. J.* **2002**, *38*, 79–86.
(16) Yue, C.; Padmanabhan, K. *Composites, Part B* **1999**, *30*, 205–217.
(17) Penn, L.; Byerley, T.; Liao, T. *J. Adhes.* **1987**, *23*, 163–185.
(18) Wu, Y.; Tesoro, G. *J. Appl. Polym. Sci.* **1986**, *31*, 1041–1059.
(19) Takayanagi, M.; Katayose, T. *J. Polym. Sci., Part A: Polym. Chem.* **1981**, *19*, 1133–1145.
(20) Takayanagi, M.; Kajiyama, T.; Katayose, T. *J. Appl. Polym. Sci.* **1982**, *27*, 3903–3917.
(21) Kim, E.; An, S.; Kim, H. *J. Appl. Polym. Sci.* **1997**, *65*, 99–107.
(22) Wu, S.; Sheu, G.; Shyu, S. *J. Appl. Polym. Sci.* **1996**, *62*, 1347–1360.
(23) Brown, J.; Chappel, P.; Mathys, Z. *J. Mater. Sci.* **1991**, *26*, 4172–4178.
(24) Law, M.; Greene, L.; Johnson, J.; Saykally, R.; Yang, P. *Nat. Mater.* **2005**, *4*, 455–459.
(25) Qin, Y.; Wang, X.; Wang, Z. *Nature* **2008**, *451*, 809–813.
(26) Li, Y.; Meng, G.; Zhang, L.; Phillip, F. *Appl. Phys. Lett.* **2000**, *76*, 2011–2013.
(27) Petrie, W.; Vohs, J. *Surf. Sci.* **1991**, *245*, 315–323.
(28) Culler, S.; McKenzie, M.; Fina, L.; Ishida, L.; Koenig, J. *Appl. Spectrosc.* **1984**, *38*, 791–795.
(29) McKenzie, M.; Culler, S.; Koenig, J. *Appl. Spectrosc.* **1984**, *38*, 786–790.
(30) Günzler, H.; Gremlich, H. *IR Spectroscopy: An Introduction*; John Wiley and Sons: New York, 2002.
(31) Carey, F. *Organic Chemistry*, 7th ed.; McGraw-Hill: New York, 2007.
(32) Beamson, G.; Briggs, D. *High Resolution XPS of Organic Polymers*; John Wiley and Sons: New York, 1992.
(33) Huang, M.; Wu, Y.; Feick, H.; Tran, N.; Weber, E.; Yang, P. *Adv. Mater.* **2001**, *13*, 113–116.
(34) Feih, S.; Wonsyld, K.; Minzari, D.; Westermann, P.; Lilholt, H. *Testing procedure for the single fiber fragmentation test*; Riso-R-1483(EN); Riso National Laboratory: Roskilde, Denmark, 2004; pp 3−28.

AM900376T